ACS OMEGA

http://pubs.acs.org/journal/acsodf

Article

Geochemical Characteristics and the Origin of Superdeep Condensates in Tarim Basin, China

Jingfei Li, Zhiyao Zhang, Guangyou Zhu,* Kun Zhao, Linxian Chi, Pengju Wang, and Yongjin Chen

Cite This: *ACS Omega* 2021, 6, 7275−7285

Read Online

ACCESS | Metrics & More | Article Recommendations | Supporting Information

ABSTRACT: A series of trace compounds (diamondoids, ethanodiamondoids, and thiadiamondoids) were detected through two-dimensional gas chromatography/time-of-flight mass spectrometry (GC × GC-TOFMS) analysis of Ordovician condensate samples from the Tazhong area. Gas chromatography-mass spectrometry (GC-MS) analysis showed that the biomarker parameters are less effective for high-maturity oils. Carbon isotope and geochemical features suggested that the gas is a high-temperature cracking gas when its temperature is higher than 170 °C. The H_2S content is 8.27%, suggesting that it is affected by thermochemical sulfate reduction (TSR). However, the geological analysis indicated that the Ordovician reservoirs do not satisfy the conditions for TSR. The high-maturity oil in the Ordovician reservoirs may generate diamondoids and ethanodiamondoids when cracking, while TSR and severe cracking occur in deep Cambrian source rocks and produce a large number of diamondoids, ethanodiamondoids, organic sulfur compounds (OSCs), etc. The secondary geochemical products that are carried up by the dry gas and migrate upward through faults and are enriched in Ordovician crude oil reservoirs. On this basis, we proposed that the condensate presented was formed by the mixing of dry gas from Cambrian oil that was altered by cracking and TSR into Ordovician in situ slightly cracked oil, therefore speculating that the favorable reservoir−seal assemblages in this area may contain abundant oil and gas resources. Consequently, improved knowledge of secondary alteration effects on the reservoir and underground fluids is vital for oil and gas prediction and exploration development in the next step.

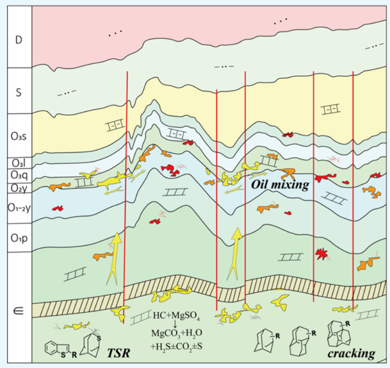

1. INTRODUCTION

The Tarim Basin is the largest oil−gas-bearing basin in China with complex geological conditions.[1−4] A large amount of condensate was discovered in well Shun7 (the Ordovician dolomite reservoir at a depth of 6820−6912 m) drilled in the Shunxi block of the Tazhong uplift in the Tarim Basin. The condensate was highly volatile, had a high content of light hydrocarbons, and contained rich geochemical information.[5,6] We used GC × GC-TOFMS, an advanced analytical technique, to identify and quantify (or investigate), paying special attention to the characteristics of abundant cagelike molecular structural compounds and OSCs in the Shun7 condensate. Diamondoids like hydrocarbon structures were formed following the thermal cracking of polycyclic hydrocarbon C−C bonds under high temperature and pressure.[7−10] Diamondoids are usually enriched in high-maturity oil and condensate, and there may be more than three cages of the diamondoid clusters (triamantanes).[9,11] As is well known, diamondoid(s) have strong thermal stability; therefore, it has been widely applied to the evaluation of maturity, biodegradation, and oil source. Similar to diamondoids, thiadiamondoids have same skeleton and distribution characteristics,[12] except that the bridgehead carbon is replaced by sulfur. The conditions for oil cracking are generally deep strata and high temperature, which continuously generate and enrich diamondoids;[12] therefore, they serve as an index to judge the degree of oil cracking.[13,14] The thia- and thiol-cage compounds are present in oil when thermochemical sulfate reduction (TSR) occurs in deep reservoirs.[2,12,15,16] It is generally considered that thiadiamondoids are typical products of TSR reactions between hydrocarbons and sulfates, which are obvious signs of TSR in oil and gas reservoirs.[17]

The TSR process results in a strong secondary alteration effect on the reservoir, leading to the intense fractionation of carbon and sulfur isotopes that convert into some acid gases such as H_2S.[18,19] There are two essential conditions for the onset of TSR, including temperatures higher than 140 °C and the existence of sulfate. TSR action can generally be divided into two stages: start-up and H_2S autocatalysis. A strong TSR effect leads to large consumption of crude oil and the continuous formation of acidic natural gas,[20] thereby promoting the transformation of the oil−gas phase state.

In recent years, with the transformation of oil and gas exploration to deep strata, a growing number of high H_2S oil

Received: October 9, 2020
Accepted: February 23, 2021
Published: March 11, 2021

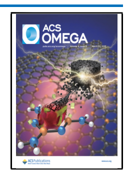

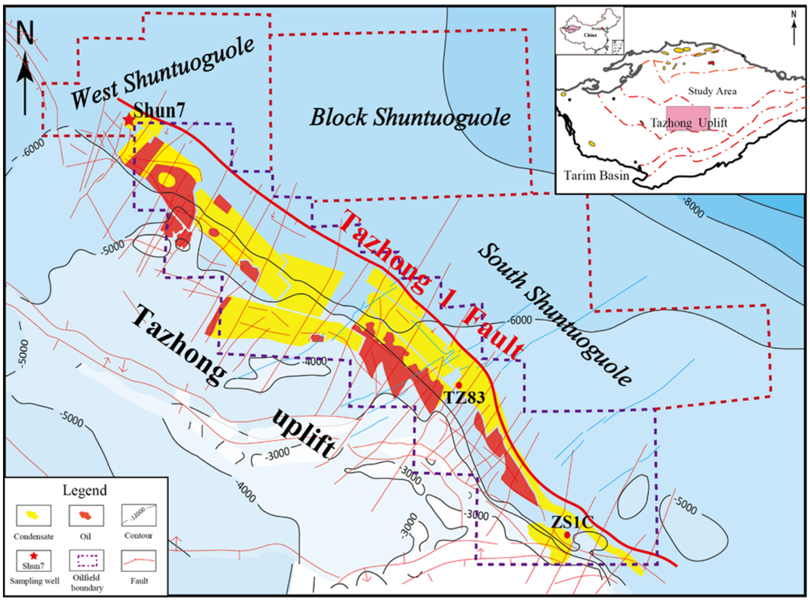

Figure 1. Structural map of the study area (modified after ref[22]).

and gas fields have been found. The relationship between H_2S and TSR, the effect of TSR, and the cracking and secondary effects of deep crude oil, etc., have become an important research area in the domain of hydrocarbon geochemistry.[21] In this work, we reported that abundant diamondoids, thiadiamondoids, and other compounds were detected in well Shun7 using high-resolution GC × GC-TOFMS and revealed the complex geological and geochemical processes in the deep layer.

2. GEOLOGICAL SETTINGS

The Tazhong I Fault condensate gas field is located in the Tazhong uplift (Figure 1). This structural zone is a long-term developed inherited paleo-uplift, which is also a major oil−gas enrichment region in the basin. Well Shun7 discussed in this article is located in the Shunxi (short for West Shuntuoguole) block in the western section of the Tazhong I Fault slope break zone, where the fault system is highly developed.[22] This area has experienced the early Caledonian (Cambrian-Middle Ordovician) sedimentary period of marine argillaceous source rocks and the carbonate platform. Middle-late Caledonian early Hercynian (Middle Ordovician-Middle Devonian) is an important period of tectonic−sediment transition, and the craton uplift was formed, followed by the uplift and erosion of Tabei uplift and the disappearance of Shuntuoguole uplift from the late Hercynian−Yanshan period (Triassic) and paleo-uplift structural finalization after the Himalayan period.[23] Well Shun7 strata include, from old to new, the lower Ordovician Penglaiba Formation (O_1p), the middle-lower Ordovician Yingshan Formation ($O_{1-2}y$), the middle Ordovician Yijianfang Formation (O_2y), the upper Ordovician Qiaerbake Formation (O_3q), Lianglitage Formation (O_3l), and the Sangtamu Formation (O_3s). Ordovician has been proved to be the main exploration and development strata by recent structural evolution research and drilling activities, with oil and gas sourced from the O_2y and the upper part of the first member of $O_{1-2}y$ (Figure 2). According to regional geological exploration research, the Ordovician platform margin karst facies reservoirs are well developed, and the main reservoirs are

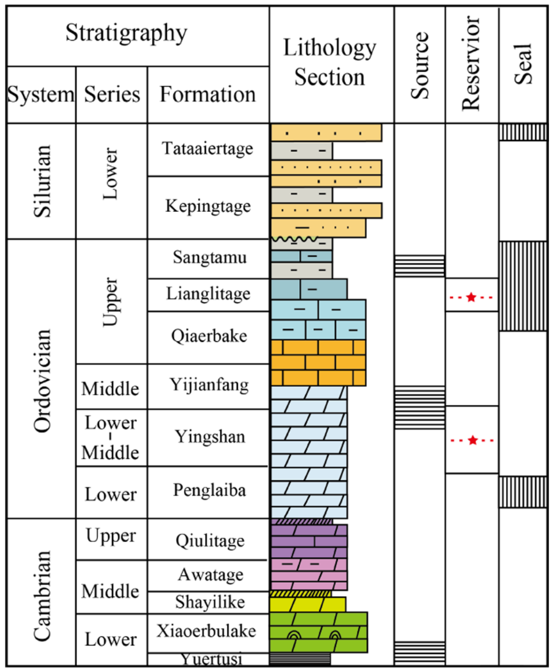

Figure 2. Comprehensive stratigraphic column of the study area (modified after ref[27]).

the Lianglitage group granite−limestone section and the Yingshan group limestone−dolomite section.

There are two sets of source rocks in this region: Cambrian marine shale and middle-upper Ordovician marine carbonate.[24] The former source rock has been recognized as the main petroleum source of the Ordovician reservoirs in the Tarim Basin with wide distribution,[25,26] and the latter are mainly formed in the middle and the west of the Manjar depression. Based on the geothermal characteristics and the tectonic evolution history, the Cambrian source rocks have reached a high mature stage and even an overmature stage, while the middle-upper Ordovician marine carbonates have high maturity. In addition, the crude oil of well Shun7 bears

https://dx.doi.org/10.1021/acsomega.0c04932
ACS Omega 2021, 6, 7275−7285

Table 1. Physicochemical Properties and Bulk Composition of Crude Oils in the Study Area

wells	depth (m)	age	density (g/cm^3) 20°C	density (g/cm^3) 50 °C	viscosity (mPa s, 50 °C)	wax (%)	sulfur (%)	resin (%)	asphaltene (%)	saturate (%)	aromatic (%)	saturate/aromatic
Shun7	6912	$O_{1-2}y$	0.775	0.756	2.84	5.82	0.13			85.72	7.23	11.86
TZ83	5685	O	0.788	0.765	3.15	12.37	0.16	1.70	0.70	72.21	11.91	6.07
ZS1C	6944	∈1x	0.927	0.908	2.18	2.70	2.57	0.45	0.08	52.87	35.72	1.48

wells	gas component (%) C_1	C_2	C_3	C_4	C_5	N_2	CO_2	dryness coefficient	carbon isotopic values (‰) $\delta^{13}C_1$	$\delta^{13}C_2$	$\delta^{13}C_3$	$\delta^{13}C_4$
Shun7	91.95	2.88	0.88	0.51	0.11	0.67	2.98	0.95	−47.8	−35.7	−29.7	−28.5
TZ83	88.50	0.71	0.12	0.10	0.06	0.69	7.34	0.99	−38.9[a]	−32.3[a]	−28.0[a]	−26.7[a]
ZS1C	67.90	0.67	0.23	0.12	0.05	4.23	21.7	0.98	−41.4	−34.7	−32.8	−28.1

[a]Data from ref.[51]

some resemblance to the geochemical characteristics of well ZS1C from the Cambrian source. Consequently, it is deemed that the oil and gas from well Shun7 originate from the Cambrian source rocks.

3. MATERIALS AND METHODS

3.1. Samples. Well Shun7 is a typical condensate with the saturation-to-aromaticity ratio of oil being 11.86. Oil−gas samples were collected from the 6820−6912 m interval at the wellhead after the separator. Geochemical and isotopic comparisons of two typical Cambrian-sourced oil samples and Well Shun7 are made, including one typical Ordovician condensate (TZ83) and a severely cracked Cambrian oil (ZS1C).

3.2. Methods. Two-dimensional gas chromatography/time-of-flight mass spectrometry (GC × GC-TOFMS) analysis was performed using a Leco Corporation instrument composed of two Agilent GC interfaces and a Pegasus 4D TOF mass spectrometer. A 50 m × 0.2 mm × 0.5 μm J&W DB-Petro silica column and a 3 m × 0.1 mm × 0.1 μm DB-17HT capillary column were used for first- and second-dimension GC, respectively. The injection port temperature is 300 °C, and the injection volume is 0.5 μL. The carrier gas is helium, and the flow rate is 1.5 mL/min. The concentrations of diamondoids, thiadiamondoids, and other compounds were quantified based on the peak areas via the internal standard method (adamantane-d_{16}; the solvent is CH_2Cl_2). More details about the procedures and conditions of the experiment can be found elsewhere.[27]

Gas chromatographic-mass spectrometry (GC-MS) biomarker analysis was performed using a TRACE GC ULTRA/DSQII instrument and a 60 m × 0.25 mm × 0.25 μm HP-5MS silica column. The initial GC oven temperature was set to 100°C, held for 5 min, and then increased to 220°C at a rate of 4°C/min; then, the temperature was set to 320°C at a rate of 2°C/min and held isothermally for 20 min. Finally, biomarker parameters were quantified through the peak area of each component.

Carbon isotopes were analyzed using a isotope ratio mass spectrometer (IRMS) connected to an Agilent 6890 gas chromatograph (GC). The $\delta^{13}C$ values are reported in per mil (‰, VPDB), with the standard deviation accuracy of 0.1‰. More details about the procedures and conditions of the experiment can be found elsewhere.[27]

4. RESULTS

4.1. Physical Characteristics and the Chemical Composition of the Condensate Oil. The density of Shun7 condensate measured at 20 °C is 0.775 g/cm^3, the measured dynamic viscosity at 50 °C is 2.84 mPa s, and sulfur and wax relative contents are 0.13 and 5.82%, respectively. The contents of saturated and aromatic hydrocarbons in Shun7 condensate oil are 85.72 and 7.23%, respectively (Table 1). Compared with TZ83 and ZS1C condensates, the content of saturated hydrocarbon in well Shun7 is significantly higher, while the aromatic hydrocarbon content is obviously low.

Natural gas in well Shun7 is a characteristic wet gas, the C_1/C_{1-4} ratio is 0.95, and the methane content is less than 95% (CH_4 is 91.95%). The $\delta^{13}C$ values of methane, ethane, and propane are −47.8, −35.7, and −29.7‰, respectively.

4.2. Geochemical Features of the Shun7 Condensate Oil. *4.2.1. GC-MS Analysis.* According to the GC-MS analysis of well Shun7 (Figure 3), the baseline is straight and has a single peak distribution, showing that the low-carbon-number *n*-alkane is dominant. The pristine/phytane (Pr/Ph) value is 1.15, which indicates the high maturity of the condensate and the weak oxidation−reduction environment.[28] As for the composition of the sterane and terpene biomarkers, due to the high crude oil maturity, the sterane and terpene series are basically cracked. In terpene (m/z = 191) biomarkers, the tricyclic terpene (TT) series are incompletely distributed, with C_{19} as the main peak and only C_{19}, C_{20}, and C_{23}TT seen, while only C_{30} and C_{29} hopane remain, and 17α(H)-trisnorhopane (Tm) completely disappeared. In sterane (m/z = 217) biomarkers, only C_{21} pregnane and a small amount of C_{27} rearranged sterane were detected, indicating that the Shun7 condensates have a high degree of maturity, leading to the breakdown of biomarker compounds.

Therefore, conventional petroleum sample analysis methods cannot meet the needs of condensate sample analysis.[5] GC × GC is a relatively new analytical technique (or tool) for separating complex mixtures; it can interpret thousands of completely separated independent compound peaks in complex mixtures such as oil, due to its higher peak capacity and resolution,[29,30] and it can be well applied to oil affected by secondary effects such as washing and thermal maturation. Combined with TOFMS, it can collect compound mass spectrum information, classify the compounds, provide an effective basis for the qualitative analysis,[5] and then use the internal standard method to quantify the compounds.

4.2.2. GC × GC-TOFMS Analysis. A few unique compound groups in Shun7 condensate were identified, more than 3899

https://dx.doi.org/10.1021/acsomega.0c04932
ACS Omega 2021, 6, 7275−7285

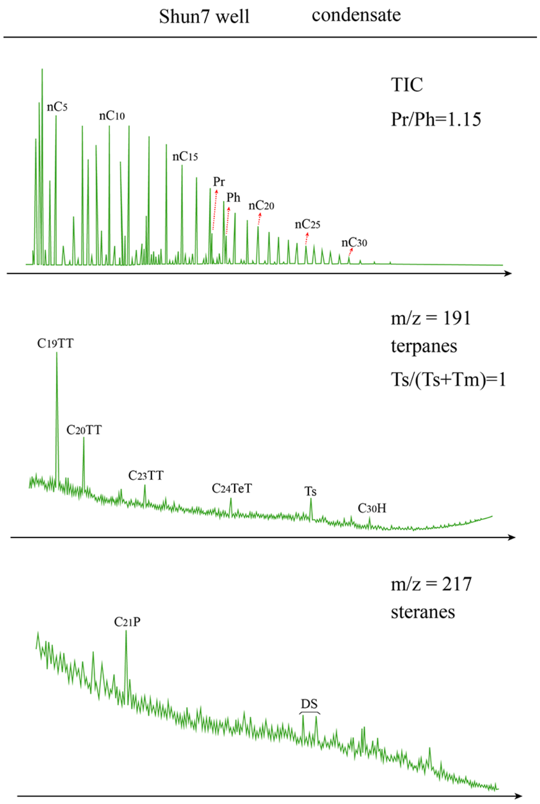

Figure 3. Representative TIC, *m/z* 191, and *m/z* 217 mass fragmentograms from GC-MS of the saturate fractions of well Shun7 condensate oils showing *n*-alkane, terpane, and sterane distributions. Note: Pr, pristane; Ph, phytane; TT, tricyclic terpene; Ts, 18*α* (*H*)-trisnorneohopane; H, hopane; P, pregnane; and DS, diasterane.

compounds with S/N > 100 (signal-to-noise ratio) were detected, and two-dimensional (2D) chromatograms and the corresponding three-dimensional (3D) peak plots were obtained using GC × GC-TOFMS analysis (Figure 4). The C_6−C_{32} hydrocarbon products including several typical series of aliphatic compounds (*n*-alkanes and cycloalkanes), aromatic compounds (benzenes, naphthalenes, phenanthrenes, etc.), diamondoids (adamantanes, diamantanes, and triamantanes), ethanoadamantanes, and organosulfur compounds (OSCs) (thiadiamondoids, benzothiophenes, dibenzothiophenes), etc. were detected. Due to the high maturity of Shun7 condensates, biomarkers, such as sterane, hopane, tricyclic terpene, etc., were not detected. The diamondoids and ethanoadamantanes detected are important indicators for oil cracking. OSCs can indicate the occurrence of TSR. The generous distributions of these compounds are separately discussed in detail below.

Diamondoids: A total of 53, 10, and 2 alkylated adamantanes, diamantanes, and triamantanes, respectively, were identified in the Shun7 condensate in different specific extracted ion chromatograms (Figure 5). Correspondingly, their concentrations were 14 135, 617, and 60 ppm (Table S1). Based on previous research, a large variety of these products were detected in petroleum by GC × GC-TOFMS analysis, but except for a few specific isomers, the exact isomeric configuration of most alkylated diamondoids cannot be clearly determined.[11,31] Compared with the severely cracked ZS1C condensate, which has the largest diamondoid cage number of 5 and the highest diamondoid content of 18.78 wt %, the diamondoids in the Shun7 condensate are of lower concentration.

Ethanodiamondoids: Ethanodiamondoids are made up of two carbons and an additional ring added to adamantanes and the higher adamantane homologues; they are diamond lattice molecules connected by ethanobridges.[32] Well Shun7 condensates also incorporated some ethanoadamantanes (Figure 6). Ethanoadamantanes (EAs) in petroleum samples are commonly ascribed to severe cracking. Figure 6a shows that 10 alkyl-ethanoadamantanes were detected in the well Shun7 condensate. The C_1−C_3 substituted ethanoadamantane groups comprised four and one isomers, respectively, with a total concentration of 319 ppm (Table S1). Figure 6b demonstrates that the content of methyl-ethanoadamantanes is the highest. Nevertheless, prior to our work, 1−3 cages of ethanoadamantanes were identified in well ZS1C.

Thiaadamantanes: Thiadiamondoids are similar to diamondoids in skeleton but the bridgehead carbon of diamondoids is replaced by sulfur. They have been identified in the Shun7 condensate but with low content. The relative content of the compound can be directly reflected in the 3D stereogram (Figure 7). The lighter the baseline background color and the more the number of convex small peaks, the lower the content of the compounds; conversely, the darker and flatter the baseline, the higher the peak and the indicative compound

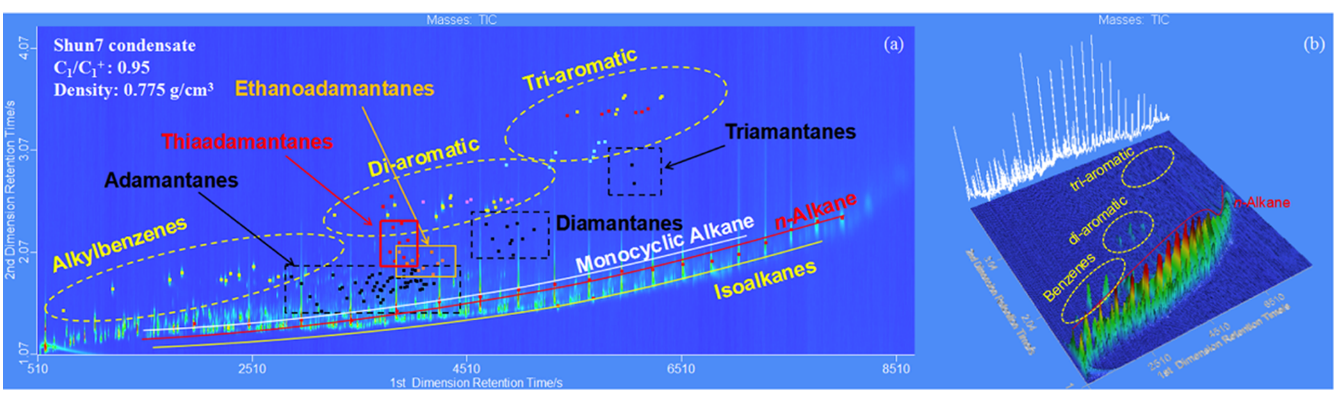

Figure 4. GC × GC-TOFMS color contour chromatograms (a) and 3D plots (b) of Shun7 condensates. Total ion current chromatogram highlighting distinctive groups of aliphatic and aromatic compounds, diamondoids, ethanoadamantanes, and thiaadamantanes; each compound series is marked with circles or boxes.

https://dx.doi.org/10.1021/acsomega.0c04932
ACS Omega 2021, 6, 7275−7285

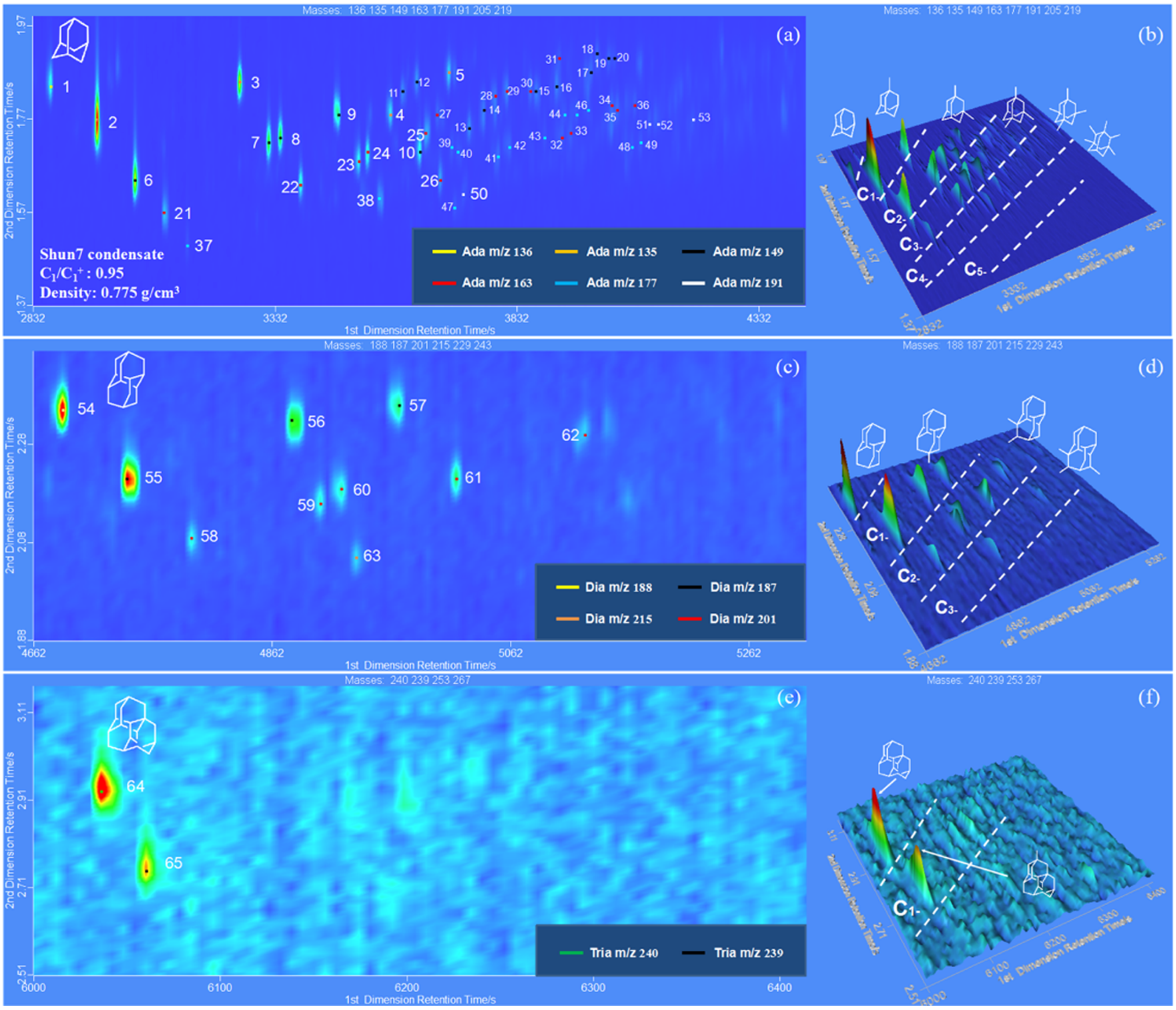

Figure 5. Diamondoid hydrocarbons with 1−3 cages highlighted by selected mass chromatograms from GC × GC-MS analysis of the Shun7 condensate: adamantane compounds highlighted by selected mass chromatograms (a) and the corresponding 3D plots (b), diamantane compounds highlighted by selected mass chromatograms (c) and the corresponding 3D plots (d), and triamantane compounds highlighted by selected mass chromatograms (e) and the corresponding 3D plots (f). Note: Ada = adamantane, Dia = diamantane, and Tria = triamantanes.

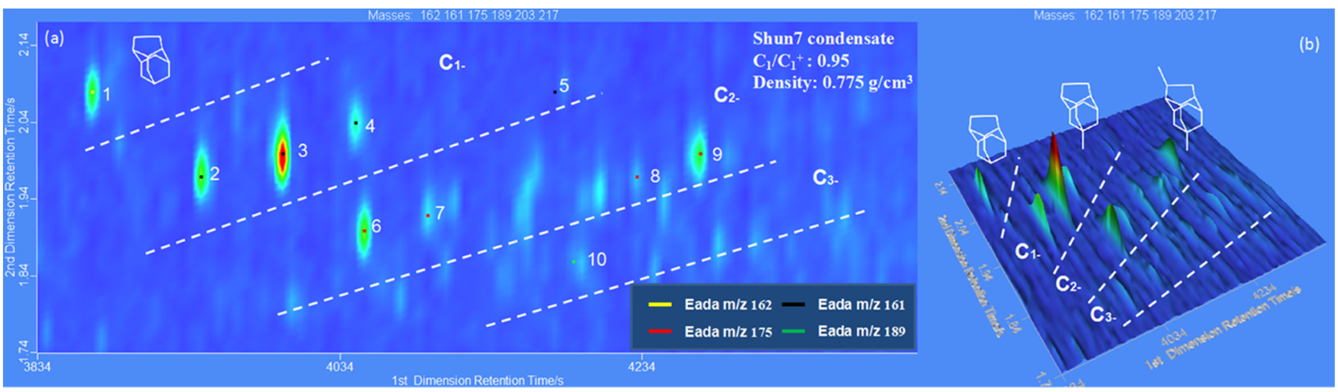

Figure 6. GC × GC-TOFMS color contour chromatograms (a) and 3D plots (b) of ethanoadamantanes in the Shun7 condensate with distinctive ions at m/z (mass-to-charge ratio) 162 + 161 + 175 + 189. Note: Eada = ethanoadamantane.

contents. As shown in the figure, 1,5-dimethyl-2-thiaadamantane is the compound with the highest content.

It can be seen from Figure 9 that other OSCs in the crude oil are benzothiophenes with m/z = 147, 161, and 175 and

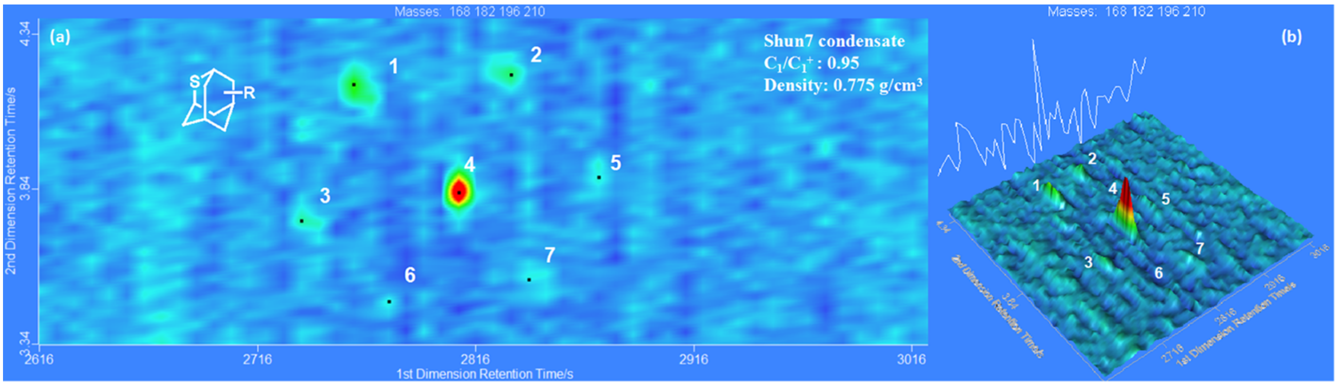

Figure 7. GC × GC-TOFMS color contour chromatograms (a) and 3D plots (b) of thiaadamantanes in the Shun7 condensate with distinctive ions at m/z 168 + 182 + 196 + 210 + 224.

Table 2. Quantitative Analysis of Diamondoids, Ethanodiamondoids, and OSCs in Well Shun7

classification	diamondoids				ethanodiamondoids
	adamantanes	diamantanes	triamantanes	total	ethanoadamantanes
content (ppm)	14135.12	616.84	59.95	14811.91	319.29

classification	OSCs			
	thiaadamantanes	benzothiophenes	dibenzothiophenes	total
content (ppm)	39.19	21.38	40.56	101.13

content of 21.38 ppm and dibenzothiophenes with m/z = 184, 198, 212 and content of 40.56 ppm (Table 2).

5. DISCUSSION

5.1. Source of Hydrocarbons.

5.1.1. Source of Diamondoids and Ethanodiamondoids. In view of the compositional characteristics and carbon isotopic and biomarker parameters from well Shun7, the condensate in this region is considered to be a high-maturity crude oil.[33] To the best of our knowledge, diamondoids have strong stability and resistance to thermal stress and it is continuously enriched at higher thermal stress levels, thus making it sensitive to reflect the thermal alteration degree of oil.[12,34,35] We have detected 65 alkyl-diamondoids and 10 alkyl-ethanoadamantanes from the Shun7 condensate, which contains the highest content of diamondoid compounds (14 812 ppm in total) in this study, and ethanoadamantanes is an isomer of adamantanes, which is a compound with extremely strong thermal stability found only in petroleum.[36] Hence, these products may reflect that the Ordovician crude oil has undergone severe cracking and high thermal evolution.

5.1.2. Source of Thiadiamondoids. Thiadiamondoids are usually considered as a typical TSR product, and their structure is analogous to diamonds.[12,37] Thiadiamondoids may be produced at high temperature and in deep strata or they may be obtained from secondary sources such as gas invasion and mixing,[38] and the high content of diamondoids in oils normally represents the occurrence of TSR. Wei et al.[17] proposed that the TSR-altered and unaltered oils could be distinguished according to the concentration of low-volatility thiadiamondoids, and the threshold was >30 ppm. Cai et al.[19] considered that the threshold for TSR modification was 28 ppm. This conclusion may not be completely true. We detected seven alkyl-thiaadamantanes, and the total content was 39 ppm in Shun7, indicating that the reservoir may have undergone TSR. Based on the comparison of the contents of diamondoids and thiadiamondoids, it was seen that the concentrations were correlated in a linear fashion (data other than Shun7 are provided by Wei et al.[17]) (Figure 8) and that

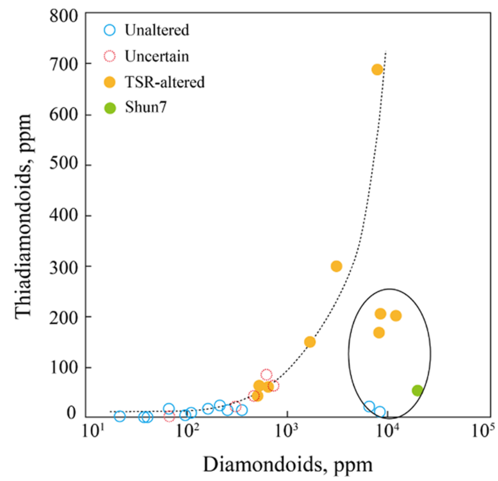

Figure 8. Relationship between thiadiamondoids and diamondoids.

the abundance of diamondoids was considerably higher than thiadiamondoids; however, the deviations of the samples in the circle can be attributed to these fluids undergoing advanced thermal cracking.[17] OSCs in Cambrian and Ordovician condensates were identified; according to the comparison chart in Figure 9, the types and contents of OSCs in the Cambrian condensate are higher, and the formation is more strongly affected by TSR.

Two conditions are required for TSR to occur: temperatures over 140 °C and evaporites.[39] In the Shunxi field, the buried depth of the Ordovician is relatively low, and the current reservoir temperature is lower than 140 °C, indicating the lack of conditions for the onset of TSR and that the OSCs may be sourced from deep strata. The Cambrian source-reservoirs are deeply buried with high formation temperatures and are

https://dx.doi.org/10.1021/acsomega.0c04932
ACS Omega 2021, 6, 7275−7285

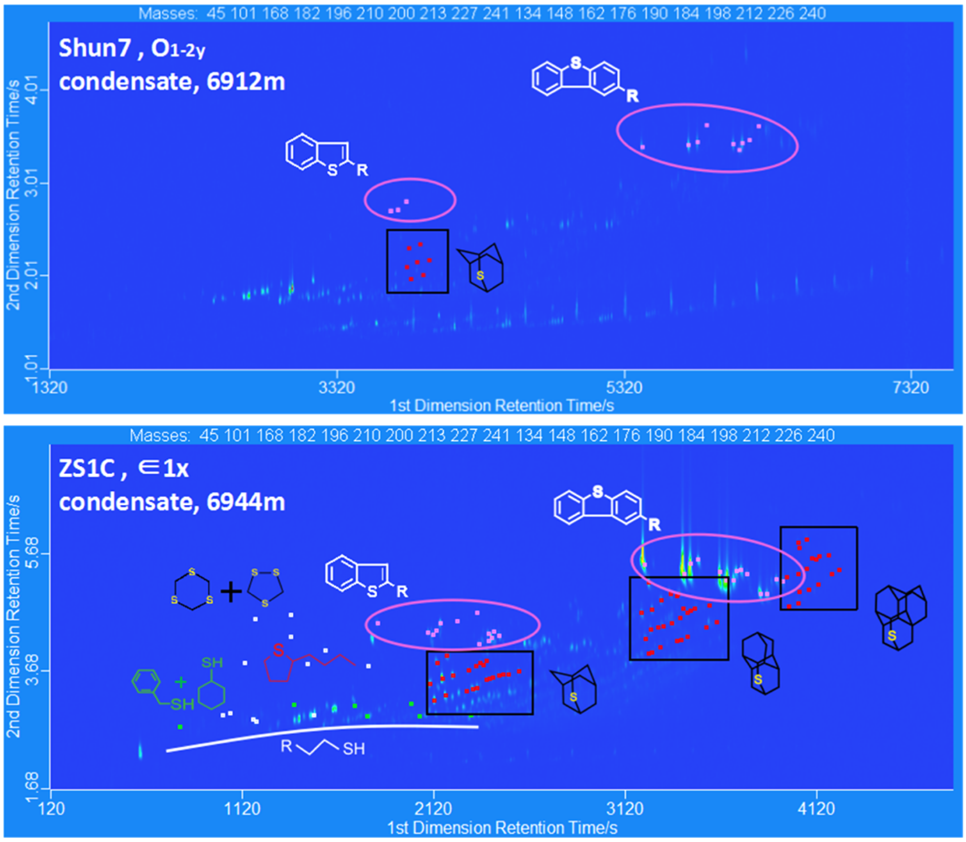

Figure 9. Distribution characteristics of sulfur compounds in Ordovician Shun7 and Cambrian ZS1C condensates.

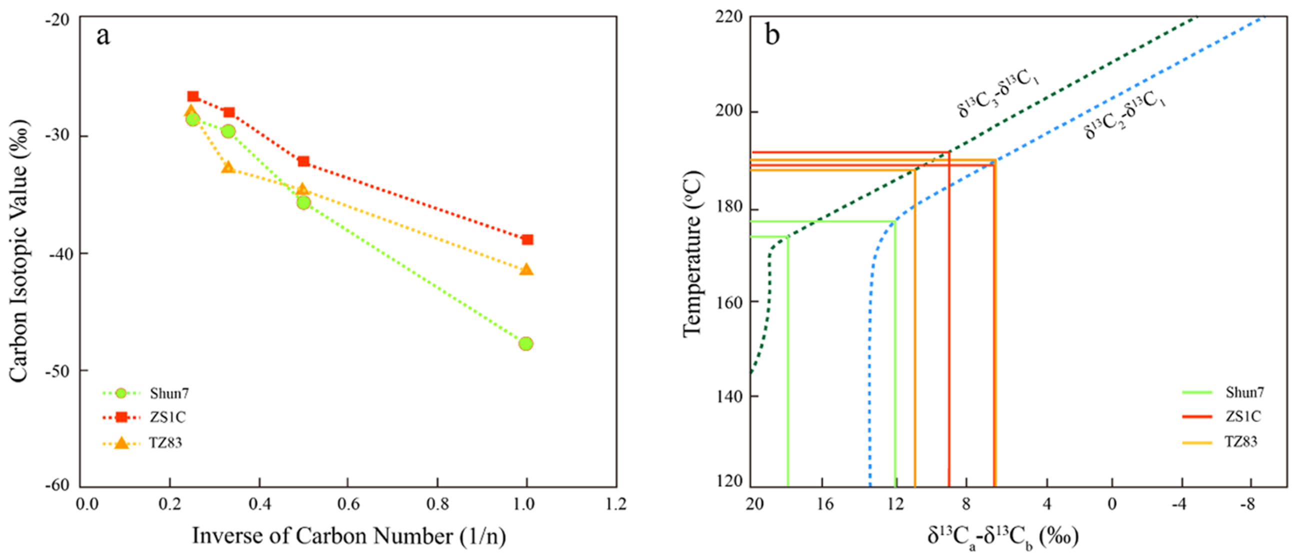

Figure 10. Relationship between the carbon number $1/n$ and $\delta^{13}C_n$ of gases (a) and the generation temperature of the condensate gas from well Shun7 (b).

associated with gypsum rock, which provides an inorganic sulfate-rich medium. Additionally, the fault system in this area is well developed and thus serves as good migration conduits. Therefore, these secondary products (diamondoids, OSCs, etc.) are considered to have been sourced from deeper Cambrian strata.

5.1.3. Source of Natural Gases. Natural gas in well Shun7 is typical wet gas; on increasing the carbon numbers, isotopic values progressively increase, showing a positive carbon number distribution sequence (Figure 10a), and $\delta^{13}C_2 < -28.0‰$, which is a typical oil-type gas.[40−42] Furthermore, the relationship between the carbon isotopes of natural gas and the generated temperature is widely applied in the gas generated by marine shale source rocks.[43] According to gases $\delta^{13}C_2-\delta^{13}C_1$ (ethane−methane carbon isotope) and $\delta^{13}C_3-\delta^{13}C_1$ (propane−methane carbon isotope), the gas generated temperature can be calculated. The results show that the value of $\delta^{13}C_2-\delta^{13}C_1$ and $\delta^{13}C_3-\delta^{13}C_1$ in well Shun7 is

https://dx.doi.org/10.1021/acsomega.0c04932
ACS Omega 2021, 6, 7275−7285

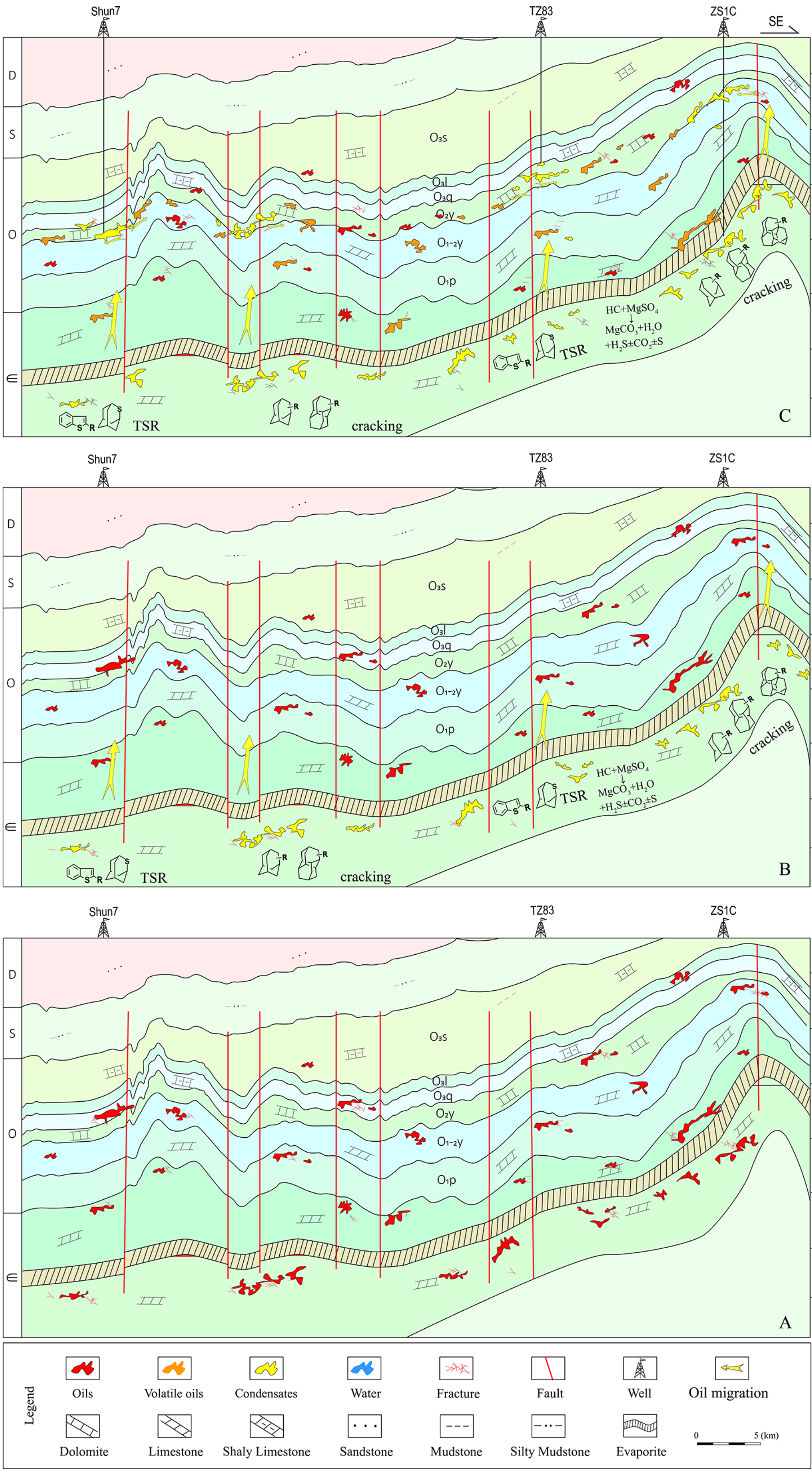

Figure 11. Schematic model showing the accumulation and alteration process of condensates in the western Tarim Basin. Stage A: Oil and gas expelled from Cambrian source rocks migrated upward into Ordovician reservoirs and formed paleo-reservoirs. Stage B: Secondary products produced as a result of the intense transformation and destruction of deep oil and gas due to oil cracking and TSR effects. Stage C: Under the action of TSR, the Cambrian dry and condensate gas are continuously mixed into the Ordovician paleo-reservoir, which gradually leads to the change of oil and gas properties and phase states of the paleo-reservoir. Note: D, Devonian; S, Silurian; O, Ordovician; ∈, Cambrian (modified after literature[47]).

https://dx.doi.org/10.1021/acsomega.0c04932
ACS Omega 2021, 6, 7275−7285

12.1 and 18.1‰, respectively. It can be seen that the temperature of the condensate gas produced in well Shun7 is higher than 170 °C (Figure 10b), which implies that it is a high-temperature cracking gas. Compared with well Shun7, wells ZS1C and TZ83 have the same trend, and even higher temperatures are generated by natural gas. Therefore, natural gas may be an oil cracking gas.[44]

TSR is a secondary alteration process in which organic matter or hydrocarbons eventually form H_2S and CO_2 through sulfate reduction.[45,46] Generally, the CO_2 content is than H_2S, which is because H_2S easily combines with heavy metal ions to form a stable metal sulfide during the formation process, resulting in high consumption of H_2S[47] and the H_2S cannot be well preserved. The content of H_2S in the natural gas of Shun7 accounts for 8.27%. Previous studies indicate that the H_2S content is ∼33.5% in Cambrian strata. Nevertheless, $\delta^{34}S$ of thiadiamondoids is heavier than that of sulfate in the Cambrian strata, and thus the $\delta^{34}S$ enrichment in thiadiamondoids should be related to the sulfur isotopic fractionation caused by TSR.[12,19] This further demonstrates that the whole or at least the major proportion of the Shun7 gases was sourced from the oil cracked gas after the Cambrian deep TSR transformation.

5.2. Impacts of Secondary Alteration. The secondary alterations of petroleum lead to the change of physical properties and phase states. Under relatively high thermal stress, oil cracks to form an oil cracking gas, which can form large-scale natural gas accumulation, and/or invade the shallow layer to change the reservoir fluid properties.[48,49] The effect of TSR reduces the critical temperature of oil cracking by 30−60 °C[50] and accelerates the cracking reaction of crude oil or heavy hydrocarbons.[2,50] However, severe TSR alteration may largely increase the sour gas (H_2S and CO_2) contents in natural gas and lead to increasing sulfur contents, the decreasing saturated/aromatic ratio, and the enrichment of nonhydrocarbons and asphaltenes in oil as well, thus consequentially affecting the chemical composition of oil and gas.

The primary Ordovician oil reservoirs in the Shun7 area are unsaturated oil reservoirs characterized as having a low gas−oil ratio (GOR), dryness coefficient, and H_2S content and are generally formed at a relatively shallow burial depth with low formation temperature. Oil cracking and TSR occurred in deeper Cambrian strata with high temperatures and enriched sulfates. TSR lowers the temperature threshold and accelerates the degree of oil cracking, and thus the Cambrian oil reservoirs cracked into the gaseous state. Such Cambrian natural gas and secondary products (diamondoids, OSCs, etc.) from cracking and TSR migrate upward through main fractures and continuously mix with oil in Ordovician reservoirs. As the degree of gas mixing increases, primary unsaturated oils gradually transition into gas-saturated oils.

5.3. Reconstruction of the Oil−Gas-Phase Changes of the Process and the Exploration Potential. Deep natural gas intrudes the Ordovician paleo-reservoir along faults. This geological condition combined with the abovementioned geochemical analysis provides an improved comprehension of the origin and postaccumulation alteration of the Shun7 condensate. The fluid-phase transformation process of the Shun7 condensate is briefly described as follows (Figure 11).

Stage A: In the paleo-reservoir-formation stage, due to the influence of fault activities, the fracture system was developed, and high-quality fracture-cave reservoirs were developed locally near the faults. Oil and gas expelled from high-quality Cambrian source rocks migrated upward along the fault system into Ordovician reservoirs and formed paleo-reservoirs with a low GOR.

Stage B: In the deep gas-source-formation stage, the Ordovician paleo-reservoir has a moderate temperature (<140 °C) and can be well preserved. The oil thermal cracking and TSR take place due to the deep Cambrian subsalt oil and gas accumulation at a high temperature (>170 °C), and sulfates in evaporite rocks are developed. Plenty of secondary products (diamondoids, ethanodiamondoids, and thiadiamondoids) are produced as a result of the intense transformation and destruction of deep oil and gas due to oil cracking and TSR effects.

Stage C: In the phase change stages, the deep Cambrian gas is continuously mixed into the Ordovician paleo-reservoir along the faults, which gradually leads to the changes in oil and gas compositions and phases of the paleo-reservoir, mainly dry and richer H_2S condensate gas, gradual enrichment of the secondary compounds indicating cracking and TSR interactions in oil, etc.

The abundance of diamondoids, ethanodiamondoids, thiadiamondoids, and fluid-phase changes observed in the Shun7 condensate may be the result of the mixing of deep Cambrian-sourced gas with shallower oils, showing that there are rich oil and gas resources in the deep Cambrian strata. In the stable structural high point of the subsalt strata of the deep Cambrian strata, there may still be a large amount of petroleum resources, mainly H_2S-rich dry gas and condensate gases, and the overlying Ordovician reservoir development areas are also key areas for hydrocarbon exploration in the next step.

6. CONCLUSIONS

Integrated geochemical and isotopic analyses on the Shun7 condensate in the Ordovician of the western Tarim Basin were performed and its origin and accumulation were unraveled. Combined with geological conditions, we put forward that in deep Cambrian strata, there may be a large amount of petroleum resources. Improved knowledge of the secondary alteration effect on the reservoir and subsurface fluids is key to oil−gas exploration development and prediction in the next step.

GC analyses show the significant loss of biomarkers in the Shun7 condensate, and thus it is classified as a high-maturity oil. An extensive series of trace molecular compounds such as diamondoids, ethanodiamondoids, and OSCs were detected by GC × GC-TOFMS. The abundant diamondoids and ethanodiamondoids reflect the severe cracking and high thermal evolution of the Ordovician crude oil, and thiadiamondoids show that Shun7 experienced TSR alteration. However, the Ordovician reservoir temperature is below 140 °C and has a shallow depth, which does not meet the conditions of TSR, indicating that they were not generated in the reservoir.

The high-temperature condition and the developed carbonate rocks in the deep Cambrian source-reservoirs are favorable for oil cracking and TSR alteration. Therefore, the secondary products (diamondoids, ethanodiamondoids, OSCs, etc.) generated by severe oil cracking and TSR in the deep Cambrian strata were carried by dry gas and migrated upward through faults to the Ordovician reservoir and were enriched.

We propose that the condensate presented was formed by the mixing of dry gas from Cambrian oil that was altered by cracking and TSR into Ordovician pre-existing oil. Meanwhile,

https://dx.doi.org/10.1021/acsomega.0c04932
ACS Omega 2021, 6, 7275−7285

the change of the fluid phase of the Ordovician paleo-reservoir may be a result of the mixing with Cambrian oil and gas, and it is speculated that the favorable reservoir−seal assemblages in this area may contain abundant oil and gas resources.

■ ASSOCIATED CONTENT

Supporting Information

The Supporting Information is available free of charge at https://pubs.acs.org/doi/10.1021/acsomega.0c04932.

Classifications, types, and concentration of diamondoid compounds in the analyzed samples (Table S1) (PDF)

■ AUTHOR INFORMATION

Corresponding Author

Guangyou Zhu − *Research Institute of Petroleum Exploration and Development, PetroChina, Beijing 100083, China;* orcid.org/0000-0002-7282-6990; Phone: +86 18601309981; Email: zhuguangyou@petrochina.com.cn

Authors

Jingfei Li − *School of Energy Resources, China University of Geosciences, Beijing 100083, China; Research Institute of Petroleum Exploration and Development, PetroChina, Beijing 100083, China*

Zhiyao Zhang − *MOE Key Laboratory of Tectonics and Petroleum Resources, China University of Geosciences, Wuhan 430074, China;* orcid.org/0000-0002-4034-0865

Kun Zhao − *School of Energy Resources, China University of Geosciences, Beijing 100083, China*

Linxian Chi − *School of Energy Resources, China University of Geosciences, Beijing 100083, China*

Pengju Wang − *School of Energy Resources, China University of Geosciences, Beijing 100083, China*

Yongjin Chen − *School of Energy Resources, China University of Geosciences, Beijing 100083, China*

Complete contact information is available at: https://pubs.acs.org/10.1021/acsomega.0c04932

Notes

The authors declare no competing financial interest.

■ ACKNOWLEDGMENTS

The authors acknowledge the PetroChina Tarim Oilfield Company for the sample collections and contributions to the data set. They thank Dr. Shengbao Shi from China University of Petroleum (Beijing) for his support with GC × GC-TOFMS technology. They are also grateful to the editor and anonymous reviewers for their constructive comments and suggestions on this article. This study was financially supported by the CNPC Scientific Research and Technology Development Project (Grant Nos. 2019B-04 and 2018A-0102).

■ REFERENCES

(1) Jin, Z. J. Particularity of petroleum exploration on marine carbonate strata in China sedimentary basins. *Earth Sci. Front.* **2005**, *12*, 15−22. [in Chinese].

(2) Hao, F.; Guo, T. L.; Zhu, Y. M.; Cai, X. Y.; Zou, H. Y.; Li, P. P. Evidence for multiple stages of oil cracking and thermochemical sulfate reduction in the Puguang gas field, Sichuan Basin, China. *Am. Assoc. Pet. Geol. Bull.* **2008**, *92*, 611−637.

(3) Zhang, S. C.; Su, J.; Wang, X.; Zhu, G. Y.; Yang, H.; Liu, K.; Li, Z. Geochemistry of Palaeozoic marine petroleum from the Tarim Basin, NW China: Part 3. Thermal cracking of liquid hydrocarbons and gas washing as the major mechanisms for deep gas condensate accumulations. *Org. Geochem.* **2011**, *42*, 1394−1410.

(4) Zhu, G. Y.; Zhang, Y.; Zhang, Z. Y.; Li, T. T.; He, N. N.; Grice, K.; Neng, Y.; Greenwood, P. High abundance of alkylated diamondoids, thiadiamondoids and thioaromatics in recently discovered sulfur-rich LS2 condensate in the Tarim Basin. *Org. Geochem.* **2018**, *123*, 136−143.

(5) Wang, P. R.; Xu, G. J.; Xiao, T. R. Environmental implications of C_5-C_{13} light fraction in crude oils. *Prog. Nat. Sci.* **2007**, *17*, 755−763.

(6) Wang, H. T.; Zhang, S. C.; Weng, N.; Li, W.; Qin, S. F.; Ma, W. L. Analysis of condensate oil by comprehensive two - dimensional gas chromatography. *Pet. Explor. Dev.* **2012**, *39*, 132−138.

(7) Petrov, A.; Arefjev, D.; Yakubson, Z. Hydrocarbons of adamantane series as indices of petroleum catagenesis process. *Org. Geochem.* **1974**, 517−522.

(8) Williams, J. A.; Bjoroy, M.; Dolcater, D. L.; Winters, J. C. Biodegradation in South Texas Eocene oil effects on aromatics and biomarkers. *Org. Geochem.* **1986**, *10*, 451−462.

(9) Lin, R.; Wilk, Z. Natural occurrence of tetramantane (C_{22} H_{28}), pentamantane (C_{26} H_{32}) and hexamantane (C_{30} H_{36}) in a deep petroleum reservoir. *Fuel* **1995**, *74*, 1512−1521.

(10) Schulz, L. K.; Wilhems, A.; Rein, E.; Steen, A. S. Application of diamondoids to distinguish source rock facies. *Org. Geochem.* **2001**, *32*, 365−375.

(11) Wei, Z. B. Molecular Organic Geochemistry of Cage Compounds and Biomarkers in the Geosphere: A Novel Approach to Understand Petroleum Evolution and Alteration. Ph.D. Dissertation, Stanford University, 2006.

(12) Wei, Z. B.; Moldowan, J.; Fago, F.; Dahl, J. E. P.; Cai, C.; Peters, K. Origins of thiadiamondoids and diamondoidthiols in petroleum. *Energy Fuels* **2007**, *21*, 3431−3436.

(13) Dahl, J.; Liu, S.; Carlson, R. Isolation and structure of higher diamondoids, nanometer-sized diamond molecules. *Science* **2003**, *299*, 96−99.

(14) Birch, S.; Cullum, T.; Dean, R.; Denyer, R. Thiaadamantane. *Nature* **1952**, *170*, 629−630.

(15) Birch, S.; Cullum, T.; Dean, R.; Denyer, R. Sulfur compounds in kerosene boiling range of Middle East crude oils. *Ind. Eng. Chem.* **1955**, *47*, 240−249.

(16) Hanin, S.; Adam, P.; Kowalewski, I.; Huc, A. Y.; Carpentier, B.; Albrecht, P. Bridgehead alkylated 2-thiaadamantanes: novel markers for sulfurisation occurring under high thermal stress in deep petroleum reservoirs. *Chem. Commun.* **2002**, 1750−1751.

(17) Wei, Z. B.; Walters, C. C.; Moldowan, J. M.; Mankiewicz, P. J.; Pottorf, R. J.; Xiao, Y. T.; Maze, W.; Nguyen, P. T. H.; Madincea, M. E.; Phan, N. T.; Peters, K. E. Thiadiamondoids as proxies for the extent of thermochemical sulfate reduction. *Org. Geochem.* **2012**, *44*, 53−70.

(18) Amrani, A.; Zhang, T.; Ma, Q.; Ellis, G. S.; Tang, Y. The role of labile sulfur compounds in thermochemical sulfate reduction. *Geochim. Cosmochim. Acta* **2008**, *72*, 2960−2972.

(19) Cai, C. F.; Amrani, A.; Worden, R.; Xiao, Q.; Wang, T.; Gvirtzman, Z.; Li, H.; Said-Ahmad, W.; Jia, L. Sulfur isotopic compositions of individual organosulfur compounds and their genetic links in the Lower Paleozoic petroleum pools of the Tarim Basin, NW China. *Geochim. Cosmochim. Acta* **2016**, *182*, 88−108.

(20) Zhang, T.; Ellis, G.; Walters, C.; Kelemen, S.; Wang, K.; Tang, Y. Experimental diagnostic geochemical signatures of the extent of thermochemical sulfate reduction. *Org. Geochem.* **2008**, *39*, 308−328.

(21) Zhu, G.; Liu, X.; Zheng, D.; Zhu, Y.; Su, J.; Wang, K. Geology and hydrocarbon accumulation of the large ultra-deep Rewapu oilfield in Tarim basin, China. *Energy Explor. Exploit.* **2015**, *33*, 123−144.

(22) Ma, A. L.; Jin, Z.; Li, J.; Zhu, X. Geochemical characteristics and origin of hydrocarbons in the well Shun-7 of western Shuntuoguole block, Tarim Basin. *Oil Gas Geol.* **2012**, *33*, 828−835. [in Chinese].

(23) Jiao, F. Significance and prospect of ultra-deep carbonate fault-karst reservoirs in Shunbei area, Tarim Basin. *Oil Gas Geol.* **2018**, *39*, 207−216. [in Chinese].
(24) Zhang, S. C.; Hanson, A. D.; Moldowan, J. M.; Graham, S. A.; Liang, D. G.; Chang, E.; Fago, F. Paleozoic oil±source rock correlations in the Tarim basin, NW China. *Org. Geochem.* **2000**, *31*, 273−286.
(25) Huang, H. P.; Zhang, S. C.; Su, J. Palaeozoic oil-source correlation in the Tarim Basin, NW China. *Org. Geochem.* **2016**, *94*, 32−46.
(26) Zhu, G. Y.; Chen, F. R.; Wang, M.; Zhang, Z. Y.; Ren, R.; Wu, L. Discovery of the lower Cambrian high-quality source rocks and deep oil and gas exploration potential in the Tarim Basin, China. *Am. Assoc. Pet. Geol. Bull.* **2018**, *102*, 2123−2151.
(27) Zhang, Z. Y.; Zhang, Y.; Zhu, G. Y.; Han, J. F.; Chi, L. X. Variations of diamondoids distributions in petroleum fluids during migration induced phase fractionation: A case study from the Tazhong area, NW China. *J. Pet. Sci. Eng.* **2019**, *179*, 1012−1022.
(28) Peters, K. E.; Walters, C. C.; Moldowan, J. M. *The Biomarker Guide: Biomarker and Isotopes in the Environment and Human History*; Cambridge University Press: Cambridge, U.K., 2005.
(29) Li, S. F.; Cao, J.; Hu, S. Z.; Luo, G. M. Characterization of compounds in unresolved complex mixtures (UCM) of a Mesoproterzoic shale by using GC×GC-TOFMS. *Mar. Pet. Geol.* **2015**, *66*, 791−800.
(30) Forsythe, J. C.; Robin, M.; Ilaria, D. S.; Richard, T.; Kate, A.; Jonathan, P.; Nelly, D. N.; Robert, K. N.; Andrew, E. P.; Stephen, K. R.; et al. Integrating comprehensive two-dimensional gas chromatography and downhole fluid analysis to validate a spill-fill sequence of reservoirs with variations of biodegradation, water washing and thermal maturity. *Fuel* **2017**, *191*, 538−554.
(31) Jiang, N.; Zhu, G. Y.; Zhang, S. C.; et al. Detection of 2-thiaadamantanes in the oil from Well TZ-83 in Tarim Basin and its geological implication. *Chin. Sci. Bull.* **2008**, *53*, 396−401. [in Chinese].
(32) Rao, S.; Sundaralingam, M.; Osawa, E.; et al. Hexacyclo [10, 3, 1, 02, 10, 03, 7, 0, 15, 09, 14] hexadecane; an ethanocongressane. *J. Chem. Soc. D* **1970**, 861−862.
(33) Dai, J. X.; Zou, C. N.; Qin, S. F.; Tao, S. Z.; Ding, W. W.; Liu, Q. Y.; Hu, A. P. Geology of giant gas fields in China. *Mar. Pet. Geol.* **2008**, *25*, 320−334.
(34) Chen, J.; Fu, J.; Sheng, G.; Liu, D.; Zhang, J. Diamondoid hydrocarbon ratios: Novel maturity indices for highly mature crude oils. *Org. Geochem.* **1996**, *25*, 179−190.
(35) Dahl, J. E.; Moldowan, J. M.; Peters, K. E.; Claypool, G. E.; Rooney, M. A.; Michael, G. E.; Mello, M. R.; Kohnen, M. L. Diamondoid hydrocarbons as indicators of natural oil cracking. *Nature* **1999**, *399*, 54−57.
(36) Zhu, G. Y.; Wang, M.; Zhang, Y.; Zhang, Z. Y. Higher Ethanodiamondoids in Petroleum. *Energy Fuels* **2018**, *32*, 4996−5000.
(37) Wei, Z. B.; Mankiewicz, P.; et al. Natural occurrence of higher thiadiamondoids and diamondoidthiols in a deep petroleum reservoir in the Mobile Bay gas field. *Org. Geochem.* **2011**, *42*, 121−133.
(38) Zhang, Z. Y.; Zhang, Y.; Zhu, G. Y.; Chi, L. X.; Han, J. Impacts of thermochemical sulfate reduction, oil cracking, and gas mixing on the petroleum fluid phase in the Tazhong area, Tarim Basin, China. *Energy Fuels* **2019**, *33*, 968−978.
(39) Worden, R.; Smalley, P.; Oxtoby, N. Gas souring by thermochemical sulfate reduction at 140 °C. *Am. Assoc. Pet. Geol. Bull.* **1995**, *79*, 854−863.
(40) James, A. Correlation of natural gas by use of Carbon isotopic distribution between hydrocarbon components. *Am. Assoc. Pet. Geol. Bull.* **1983**, *67*, 1176−1191.
(41) Chung, H.; Gormly, J.; Squires, R. Origin of gaseous hydrocarbons in subsurface environments theoretical considerations of carbon isotope distribution. *Chem. Geol.* **1988**, *71*, 97−103.
(42) Dai, J. X.; Zou, C. N.; Li, J.; Ni, Y. Y.; Hu, G. Y.; Zhang, X. B.; Liu, G. Y.; Yang, C.; Hu, A. P. Carbon isotopes of Middle − Lower Jurassic coal - derived alkane gases from the major basins of northwestern China. *Int. J. Coal Geol.* **2009**, *80*, 124−134.
(43) Rooney, M. A.; et al. Modeling thermogenic gas generation using carbon isotope ratios of natural gas hydrocarbons. *Chem. Geol.* **1995**, *126*, 219−232.
(44) Worden, R. H.; Smalley, P. C. H_2S-producing reactions in deep carbonate gas reservoirs: Khuff formation, Abu Dhabi. *Chem. Geol.* **1996**, *133*, 157−171.
(45) Machel, H. G.; Krouse, H. R.; Sassen, R. Products and distinguishing criteria of bacterial and thermochemical sulfate reduction. *Appl. Geochem.* **1995**, *10*, 373−389.
(46) Worden, R. H.; Smalley, P. C.; Cross, M. The influence of rock fabric and mineralogy on thermochemical sulfate reduction: Khuff Formation, Abu Dhabi. *J. Sediment. Res.* **2000**, *70*, 1210−1221.
(47) Zhu, G. Y.; Zhang, Z. Y.; Milkov, A. V.; Zhou, X. X.; Yang, H. J.; Han, J. F. Diamondoids as tracers of late gas charge in oil reservoirs: Example from the Tazhong area, Tarim Basin, China. *Fuel* **2019**, *253*, 998−1017.
(48) Zhang, Z. Y.; Zhu, G. Y.; Zhang, Y. J.; Han, J. F.; Li, T. T.; Wang, E.; Greenwood, P. The origin and accumulation of multi-phase reservoirs in the east Tabei uplift, Tarim Basin, China. *Mar. Pet. Geol.* **2018**, *98*, 533−553.
(49) Zhou, X. X.; Lü, X. X.; Zhu, G. Y.; Cao, Y. H.; Yan, L.; Zhang, Z. Y. Origin and formation of deep and superdeep strata gas from Gucheng- Shunnan block of the Tarim Basin, NW China. *J. Pet. Sci. Eng.* **2019**, *177*, 361−373.
(50) He, K.; Zhang, S. C.; Mi, J. K.; Mao, R.; Shuai, Y. H.; Bi, L. N. Effects of thermochemical reduction initiated by different sulfates on the generation of oil cracking gas. *Acta Petrol. Sin.* **2013**, *34*, 720−726.
(51) Zhu, G. Y.; Zhang, B. T.; Yang, H. J.; Su, J.; Han, J. F. Origin of deep strata gas of Tazhong in Tarim Basin, China. *Org. Geochem.* **2014**, *74*, 85−97.

https://dx.doi.org/10.1021/acsomega.0c04932
ACS Omega 2021, 6, 7275−7285